COMPRESSION, FLEXURE AND WEAR BEHAVIOURS OF ALUMINIUM 6082-T6 ALLOY

Saurav SAGAR[1], Nilamber K. SINGH[2], Nityanand S. MAURYA[3]

The objective of the paper is to study compression, flexure and wear behaviours of Al6082-T6 alloy. In 6xxx series, this alloy has the highest strength. A Zwick/Roell 250 kN electromechanical universal testing machine is used for compression (0.001-0.1 s^{-1}) and flexure (1-100 mm/min) tests using different fixtures. Sensitivity of the alloy is obtained to the compressive and flexural loadings, whereas, the dependency of material properties is observed on the specimen geometry. Johnson-Cook material model is in good agreement with the experimental results obtained under above loadings. Wear tests for the alloy are performed on ball-on-disc tribometer under varying normal loads 10-30 N, sliding speeds 200-400 rpm and temperatures 25-200 ℃ at constant time 30 minutes. Worn surfaces analyses of tested specimens are done using scanning electron microscope.

Keywords: Al6082-T6, strain rate, compression, flexure, wear and scanning electron microscope.

1. Introduction

Aluminium alloys are widely used structural materials for construction, transportation, aerospace and marine because of their improved mechanical and tribological characteristics. High strength to density ratio, good ductility, good fabrication response and excellent corrosion resistance of the alloys attracted engineers for designing lightweight structures. Researchers have studied the behaviour of different grades of aluminium alloys under various loading conditions. Wang and Jiang [1] studied the dynamic compressive behaviour of Al2024-T4 and Al7075-T6 alloys with strain rates 2000 s^{-1} and 2500 s^{-1} at low temperatures (-150 to 27 ℃). The flow stress is found increasing with decreasing temperature, while the low temperatures have little effect on their strain hardening. Mondal et al. [2] observed that on addition of 1 wt.% Ca in Al7178 alloy, flow stress improves by nearly 35–50 MPa under compression (0.01 s^{-1}). Negative sensitivity of Al6063 was found by Ye et al. [3] at 0.001-0.8 s^{-1} (quasi-static) and positive sensitivity at 1500-3500 s^{-1} (dynamic) compression tests in

[1]Res. Scholar, National Institute of Technology Patna, India, e-mail: sauravsagar2k9@gmail.com
[2]Assoc. Professor, National Institute of Technology Patna, India, e-mail: nilambersingh@nitp.ac.in
[3]Professor, National Institute of Technology Patna, India, e-mail: nsmaurya@nitp.ac.in

artificial aged and solution treated conditions. The ANN (artificial neural network) model predicted the flow stress of Al–Cu–Mg–Ag precisely at 0.001-10 s^{-1} and 340–500 ℃, as observed by Lu et al. [4]. Wang et al. [5] observed the energy dissipation capacity of the closed-cell Al-alloy foam (Mg: 0.45%, Ca: 0.52%, Ni: 0.21%, Al: balanced, in wt.%) improved at 60% strain by nearly 61% for 10^{-3} to 450 s^{-1} increased strain rate. Linul et al. [6] found that the closed-cell aluminium alloy foam of A356 alloy performs better in axial loading direction compared to lateral one on increasing temperature (25-450 ℃) at constant crosshead speed of 10 mm/min. Aluminium bronze is sensitive at 0.01-10 s^{-1} and 500-800 ℃ as investigated by Xu et al. [7] using simulator isothermal hot compression tests. Prakash et al. [8, 9] found negative sensitivity in Al5052-H32 and positive sensitivity in Al2014-T6 to loading rates (tension, compression and flexure). Li et al. [10] presented the flexural properties (four-point bending) of 7A04-T6 alloy. Zhang et al. [11] observed improved flexural performance of aluminium (reinforced) and glass composite beams compared to the unreinforced ones. Akram et al. [12] improved the wear properties of Ni-Al bronze and Al2014-T6 alloy. Razzaq et al. [13] observed the wear resistance of the composite (AA6063 and fly ash) superior to the alloy without reinforcement. Recently, the authors have published the strain rate behaviour and notch sensitivity of the alloy Al6082-T6 under tensile loads (Sagar et al. [14]). In this paper, the authors have discussed the compression, flexure and wear behaviours of Al6082-T6 alloy.

2. Experiments

The 12 mm diameter cylindrical rods and 6 mm thick flat sheets of Al6082-T6 alloy are purchased for test specimens. Chemical composition (in wt. %) of the alloy is Cr: 0.25, Cu: 0.10, Fe: 0.50, Mg: 1.00, Mn: 0.80, Si: 1.00, Ti: 0.10, Zn: 0.20, Al: balance. Compressive specimens (diameter, D = 10 mm) of L/D = 0.4, 0.8 and 1.2 are prepared corresponding to the lengths (L_s) 4 mm, 8 mm and 12 mm respectively, for examining the effects of their geometry on the material properties. Flexural specimens (flat) of thickness (h) 6 mm, width (w) 10 mm and span lengths, S (100 mm, 150 mm and 200 mm) are used for three-point bending tests (impactor radius 10 mm). Hemispherical support of 25 mm radius is used to support the flexural specimens at their ends and the impactor speed (V) is considered same as the crosshead speed. A computer operated (software: testXpert) 250 kN Zwick/Roell electromechanical universal testing machine (UTM) is used for the experiments (Figs.1 a and b) at room temperature 25 ℃. The obtained engineering data of stress-strain are converted into their true values using eqns. (1) and (2).

$$\text{Compression: True Stress, } \sigma_{cT} = \sigma_{cs}(1 - \varepsilon_{cs}) \text{ and True Strain, } \varepsilon_{cT} = -ln(1 - \varepsilon_{cs}) \quad (1)$$

$$\text{Flexure: True Stress, } \sigma_{fT} = \sigma_{fs}(1 + \varepsilon_{fs}) \text{ and True Strain, } \varepsilon_{fT} = ln(1 + \varepsilon_{fs}) \quad (2)$$

Where, σ_{cs} and σ_{fs} are engineering stresses, while, ε_{cT} and ε_{fs} are engineering strains under compression and flexure respectively.
Wear behaviour of the alloy is studied on a ball-on-disc tribometer (Fig.1c). Wear tests are carried out for varying normal loads 10-30 N, sliding speeds 200-400 rpm and temperatures 25-200 ℃ for constant time 30 minutes on a circular track about 6 mm in diameter on the wear specimen (20 mm × 20 mm × 4 mm) by a stainless-steel ball of diameter 10 mm. Worn surfaces analyses of tested specimens are done using scanning electron microscope. In this paper, each data point corresponds to the average of three experimental results.

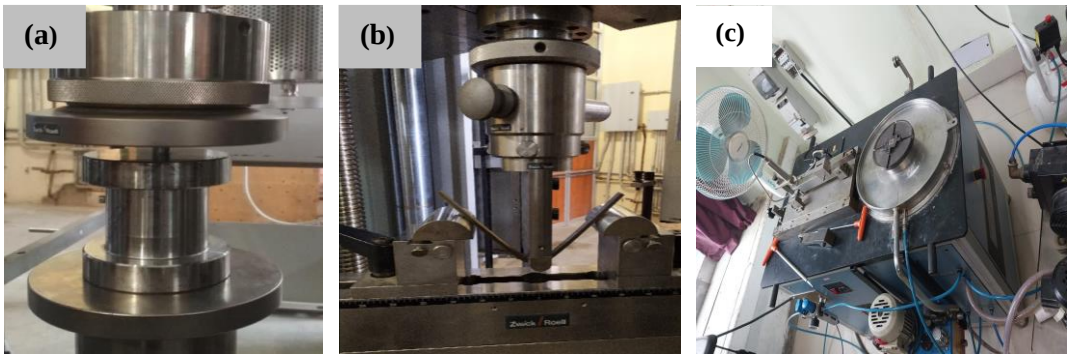

Fig. 1 Experiments on (a) UTM under compressive loads (b) UTM under flexural loads and (c) ball-on-disc tribometer for wear properties.

3. Results and discussion

3.1 Compression behaviour

Compression tests (0.0001-0.1 s^{-1}) data for the cylindrical specimens of Al6082-T6 alloy are analyzed (Fig. 2 and Table 1). Stress-strain curve (smooth yielding) is found sensitive to the strain rates and *L/D* ratios (0.4, 0.8 and 1.2). The specimens are not fractured in their 50% compression. For 0.0001 to 0.1 s^{-1} increased rate (*L/D* = 1.2), the yield strengths, YSs (at 0.2% offset strain) are improved by 10.77% (engineering) and 12.08% (true), whereas, the ultimate compressive strength (UCS) under 50% compression, improved by 11.20% (engineering) and 11.37% (true). The compressive toughness/energy dissipation is enhanced by 11.98%. As materials may be positive sensitive, negative sensitive or insensitive to the strain rates [15-18], the material properties may increase, decrease or remain almost constant with increasing strain rates. Also, the stiffness of used machine and test specimens affects the material properties. Slope of the tangent at yield point of the stress-strain curve increases with increasing *L/D* ratio (0.4 - 1.2). When the ratio *L/D* increases from 0.4 to 1.2, the energy dissipation increases by 2.36% at 0.0001 s^{-1}, 44.85% at 0.001 s^{-1}, 22.92% at 0.01 s^{-1} and

31.35% at 0.1 s^{-1}. Barreling effects are high for *L/D* = 1.2 and low for *L/D* = 0.4. No buckling effects are observed in the specimens. Hopperstad et al. [19] observed that on increasing the ratio (10.5-30.5) of width to thickness of the Al6082-T6 alloy plate, flow stress decreases for both T4 and T6 tempers under compression. Compressive strength is more for T6 tempered alloy compared to the T4 tempered alloy. Also, the elastic modulus of the alloy under compression is 10-20% lower than that under tension. Xu et al. [7] observed that on increasing temperature (200-400 °C), the flow stress decreases. Qian et al. [20] investigated that on uniaxial compression, the activation energy in the Al6082 alloy increases with increasing Mn contents (0.05–1.0 wt%). Torić et al. [21] confirmed that the flow stress decreases with increasing temperature (20 °C to 350 °C) at uniform stress rate 10 MPa/s. Zhang and Baker [22] observed that the AA6082-T4 and AA6082-O alloys follow the phenomenon of dynamic precipitation and coarsening during deformation at 0.005-0.09 s^{-1} and 300-500 °C.

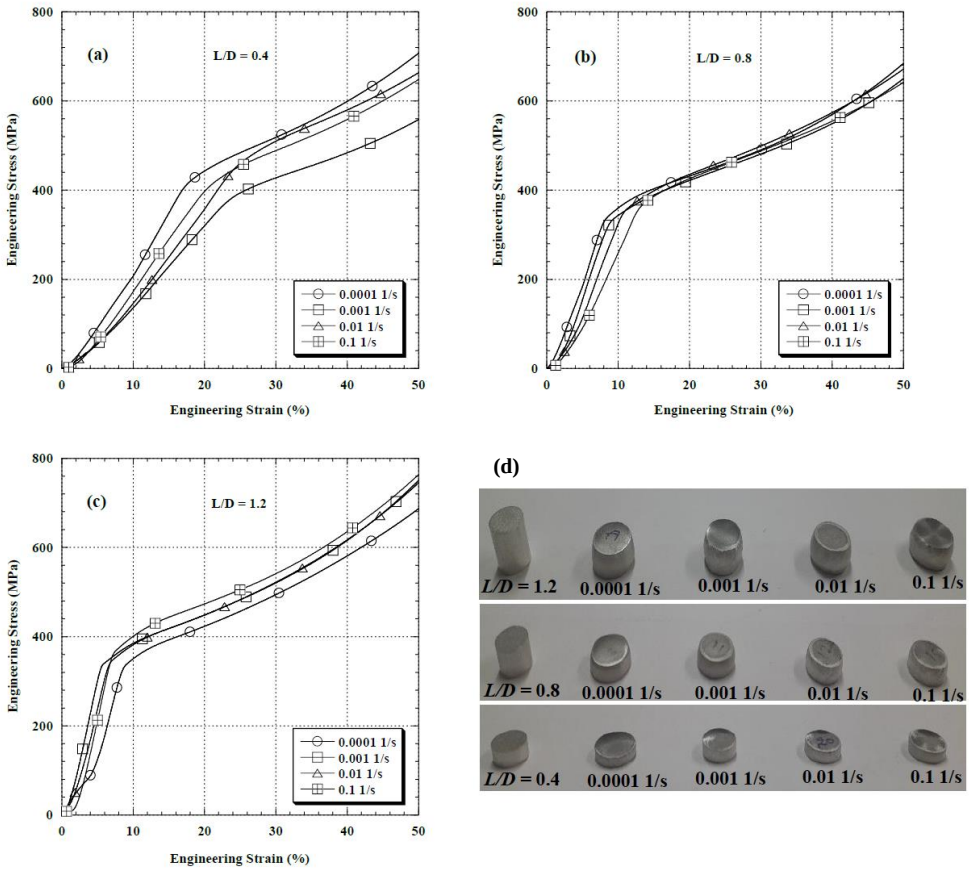

Fig. 2 Comparison of stress-strain curves under compression for (a) *L/D* = 0.4 (b) *L/D* = 0.8 and (c) *L/D* = 1.2, with (d) deformed specimens (here, s^{-1} = 1/s).

Table 1

Compressive properties of Al6082-T6 at different strain rates

L/D Ratio	Strain Rate (s^{-1})	Engineering stress-strain curves		Compressive Toughness at 50% compression (MJ/m^3)	True stress-strain curves	
		YS (MPa)	UCS at 50% compression (MPa)		YS (MPa)	UCS at 50% compression (MPa)
0.4	0.0001	410 ± 2	707 ± 5	212 ± 1	340 ± 3	359 ± 2
	0.001	372 ± 2	558 ± 2	165 ± 0.3	286 ± 3	291 ± 2
	0.01	448 ± 2	663 ± 3	192 ± 0.3	340 ± 3	348 ± 2
	0.1	400 ± 2	649 ± 3	185 ± 0.3	319 ± 2	335 ± 2
0.8	0.0001	326 ± 2	684 ± 5	220 ± 1	300 ± 2	342 ± 2
	0.001	321 ± 3	650 ± 3	211 ± 0.3	293 ± 3	329 ± 2
	0.01	345 ± 2	672 ± 2	215 ± 0.3	309 ± 3	344 ± 3
	0.1	359 ± 2	643 ± 3	204 ± 0.3	313 ± 2	333 ± 2
1.2	0.0001	325 ± 2	687 ± 5	217 ± 1	298 ± 2	348 ± 2
	0.001	332 ± 3	750 ± 2	239 ± 0.2	314 ± 4	369 ± 3
	0.01	338 ± 2	745 ± 3	236 ± 0.2	316 ± 3	370 ± 3
	0.1	360 ± 2	764 ± 3	243 ± 0.3	334 ± 3	381 ± 3

3.2 Flexure behaviour

Flexure behaviour (Fig. 3a and Table 2) of the alloy at different conditions shows its sensitivity to the crosshead speeds (1-100 mm/min). The YS (yield strength) changes faster than the UFS (ultimate flexural strength). The dissipation energy varies nearly 76-80 MJ/m^3 for span length 150 mm at speeds 1-100 mm/min, whereas, 38-79 MJ/m^3 for span lengths 100-200 mm at speed 100 mm/min. Flow stress improves with reducing span length (Fig. 3b). Crack is developed on tension side of each specimen. On increasing speed/strain rate and decreasing span length, the size of the crack increases. The decreased UFS and energy dissipation for span length 150 mm at 100 mm/min is due to large crack developed in tension side during its bending. Influence of orientation (flat and transverse) is more on UFS compared to that on YS. The increased ductility by 18.66% and energy dissipation by 15.79% of the alloy is obtained in transverse orientation of the specimen having span length 150 mm at crosshead speed 100 mm/min (Fig. 3c). No yielding instability is found on the stress-strain curve of the alloy (Fig. 3a-c). Leoni et al. [23] found more flexural strength and ductility in gas metal arc AA6082-T6 weldments than the base alloy at speed 1 mm/min using filler material of 1.2 mm diameter wire of AA5183 alloy. Troiani and Zavatta [24] observed improved fatigue life (1.7 to 3.3 times longer) of notched components of the Al6082-T6 alloy in three-point bending tests through the laser peening without coating. Zhao and Zhai [25] studied that the failure of the circular hollow pipes of the Al6082-T6 alloy depends on diameter-to-thickness ratios during four-point bending. Sert et al. [26] studied the three-point bending behaviour of different tempers Al6082 tubes and found that temper T6 is superior in specific energy

absorption (SEA), whereas T4 and O have approximately identical SEA capacities. Equivalent strain rate in Table 2 is determined by the eqn. (3) [27, 28], the variables are defined in Section 2.

Flexural strain Rate: $\dot{\varepsilon}_f = \frac{6Vh}{S^2}$ (3)

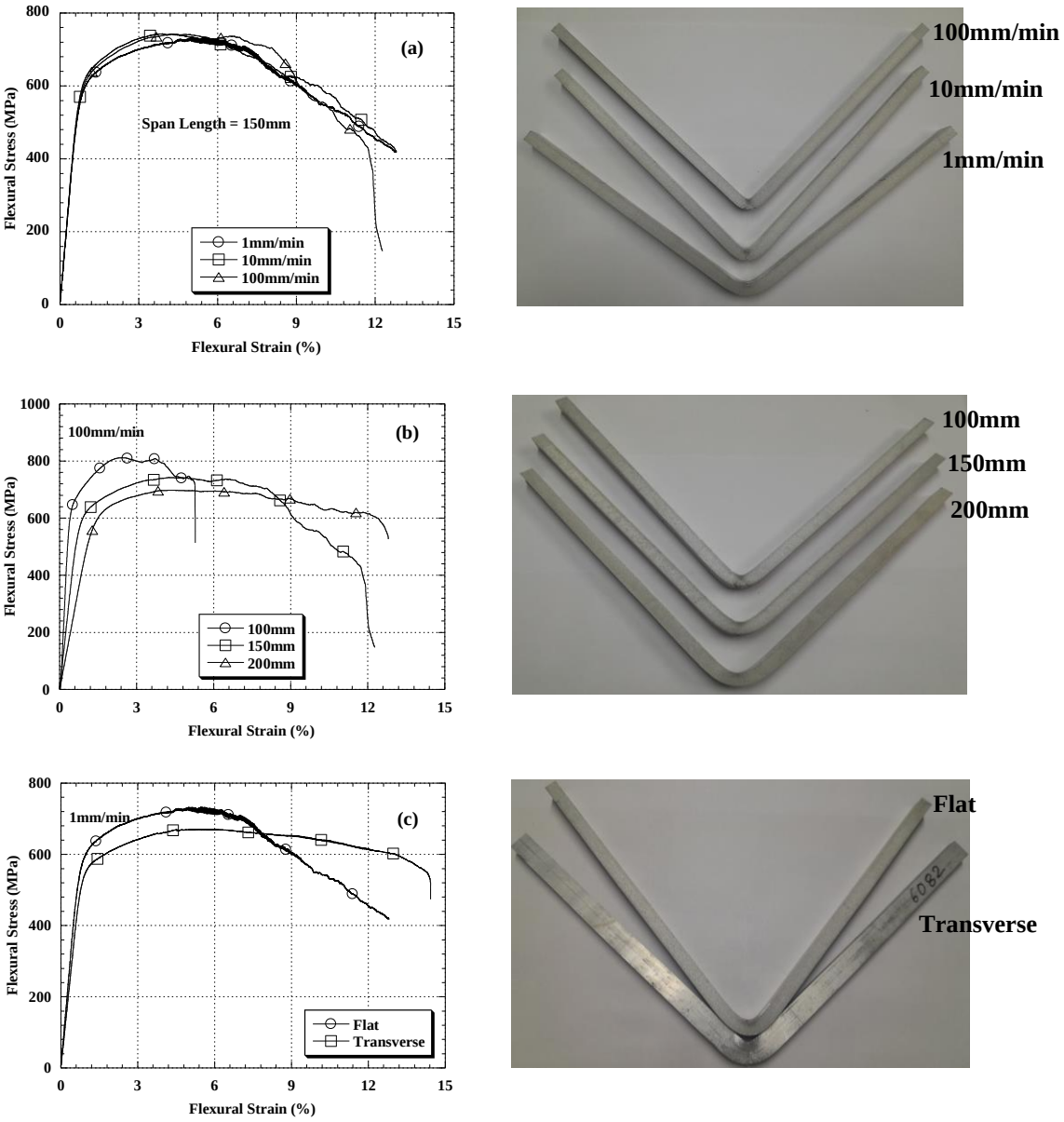

Fig. 3 Comparison of flexural stress-strain curves with deformed specimens at different (a) crosshead speeds for 150 mm span length (b) span lengths for constant speed 100 mm/min and (c) orientations of flexural specimens.

Table 2

Flexural properties of Al6082-T6 at different strain rates

Span Length (mm)	Speed (mm/min)	Equivalent strain rate (s^{-1})	Engineering stress-strain curves			Flexure Toughness (MJ/m^3)	True stress-strain curves	
			YS (MPa)	UFS (MPa)	Total Elongation (%)		YS (MPa)	UFS (MPa)
100	100	0.006	662 ± 4	811 ± 4	5.28 ± 0.3	38 ± 2	666 ± 4	831 ± 5
150	1	0.0000267	590 ± 3	733 ± 3	12.8 ± 0.2	78 ± 2	596 ± 3	773 ± 3
150	10	0.000267	613 ± 2	743 ± 3	12.8 ± 0.3	80 ± 1	619 ± 3	772 ± 3
150	100	0.00267	603 ± 3	742 ± 3	12.27 ± 0.2	76 ± 2	608 ± 3	774 ± 4
200	100	0.0015	605 ± 3	698 ± 4	12.8 ± 0.3	79 ± 2	614 ± 4	728 ± 5
150 (T)	100	0.0044	553 ± 3	671 ± 4	14.56 ± 0.3	88 ± 2	559 ± 4	707 ± 5

3.3 *Material model*

The Johnson-Cook (JC) model for compression (L/D = 1.2) and flexure can be represented by the eqn. (4) [27-29];

$$\sigma = \left(A + B\varepsilon_p^n\right)(1 + C \ln \dot{\varepsilon}^*) \quad (4)$$

In compression, the parameters are, A = 298 MPa, B = 63.108, $n = 0.34905$ and C = 0.02641 at 0.001 s^{-1}; 0.013664 at 0.01 s^{-1}; 0.015673 at 0.1 s^{-1}, whereas, in flexure, the parameters are, A = 666 MPa, B = 8359, $n = 1.2517$ and C = -0.11274 at 10 mm/min; -0.067226 at 100 mm/min. These parameters are determined using curve fitting method. Here, σ = true stress, ε_p = true plastic strain, $\dot{\varepsilon}^* = \frac{\dot{\varepsilon}}{\dot{\varepsilon_0}}$ = the dimensionless strain rate ($\dot{\varepsilon_0} = 0.0001$ s^{-1} is the reference strain rate under compression and $\dot{\varepsilon_0} = 1$ mm/min is the reference speed under flexure). The JC models can represent the flow stresses under compression and flexure, as shown in Fig. 4.

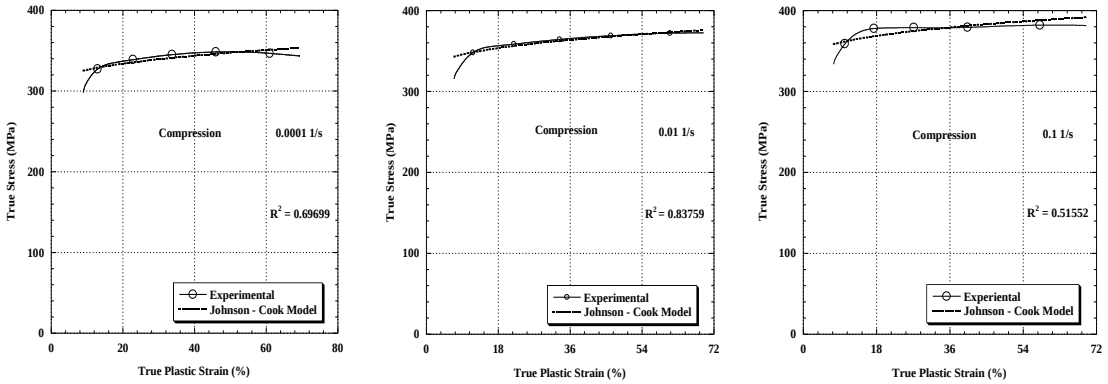

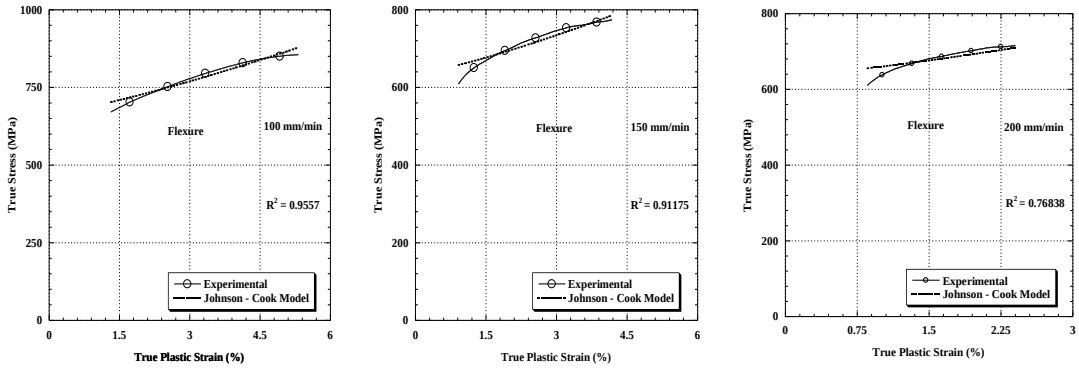

Fig. 4: Prediction of flow stresses by JC model at different strain rates.

3.4 *Wear behaviour*

Experimental data of wear tests conducted on ball-on-disc tribometer under varying normal loads 10-30 N, sliding speeds 200-400 rpm and temperatures 25-200 ℃ for constant time 30 minutes, are analyzed. Worn-out surfaces with SEM images (250X magnification) are shown in Fig. 5 and the wear properties under different conditions are given in Table 3. It is found that the increasing sliding speed or the increasing normal load on the ball, increases the wear loss and wear rate of the alloy. Also, the wear loss and wear rate are increased on increasing temperature upto 100 ℃ and then decreased at 200 ℃. The maximum wear loss and wear rate are obtained at maximum applied normal load (30 N), whereas the minimum wear loss and wear rate are found at highest temperature (200 ℃). Thus, the nature of worn-out surfaces correlates with the experimental results obtained in Table 3. Variations in friction force with sliding time under different conditions are shown in Fig. 6. As expected, the increasing applied load (10-30 N) on the ball, increases the friction force with time. When the sliding speed increases from 200 rpm to 300 rpm, the friction force increases and then decreases at the speed 400 rpm due to generation of temperature which softens the material. Also, at maximum temperature 200 ℃, the friction force decreases compared to that at 100 ℃ due to thermal softening. Friction force is maximum for applied load and minimum for sliding speed. Compositing with graphite Gr (Sharma et al. [30]), yttria particles (Zhang and Li [31]) and ZrO_2 ceramic particles (Yuvaraj [32]), the wear performance of the Al6082 alloy can be improved. The wrought Al6082 alloy has dominant wear behaviour against 410 stainless steel in a combined solution of sodium chloride and sodium molybdate dihydrate (Panagopoulos et al. [33]).

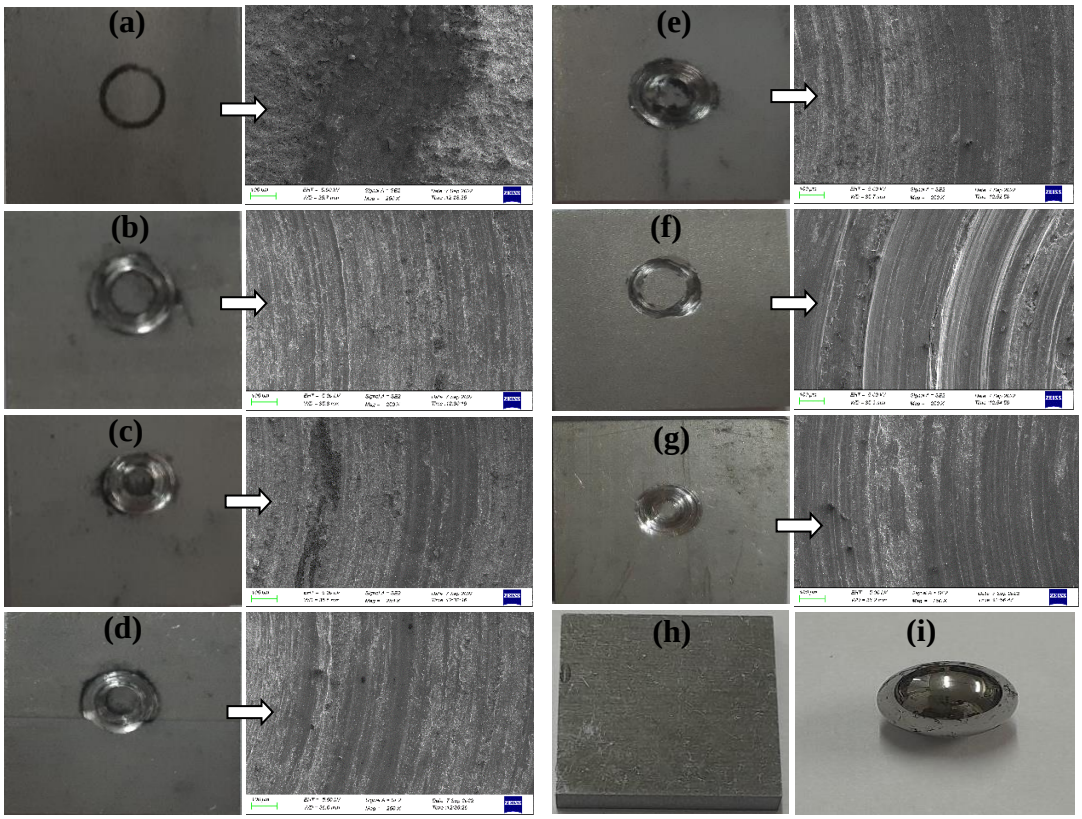

Fig. 5 Photographs of worn-out surfaces with their SEM Images at (a) 200 rpm, 10 N, 30 minutes (b) 300 rpm, 10 N, 30 minutes (c) 400 rpm, 10 N, 30 minutes (d) 400 rpm, 20 N, 30 minutes (e) 400 rpm, 30 N, 30 minutes (f) 200 rpm, 10 N, 30 minutes, 100 ℃ and (g) 200 rpm, 10 N, 30 minutes, 200 ℃; photographs of (h) wear specimen and (i) used steel ball during wear tests.

Table 3

Wear properties at different conditions

Conditions	Initial Mass of the wear Specimen (gm)	Final Mass of the Specimen after wear (gm)	Wear Loss (gm)	Wear Rate (gm/sec)
200 rpm, 10 N, 30 minutes, 25 ℃	3.6492	3.4275	0.2217	1.2316×10^{-4}
300 rpm, 10 N, 30 minutes, 25 ℃	3.4911	3.2064	0.2847	1.5816×10^{-4}
400 rpm, 10 N, 30 minutes, 25 ℃	3.7475	3.4150	0.3325	1.8472×10^{-4}
400 rpm, 20 N, 30 minutes, 25 ℃	4.0005	3.4323	0.5682	3.1566×10^{-4}
400 rpm, 30 N, 30 minutes, 25 ℃	3.7831	3.0617	0.7214	4.0077×10^{-4}
200 rpm, 10 N, 30 minutes, 100 ℃	3.1415	2.4869	0.6546	3.6366×10^{-4}
200 rpm, 10 N, 30 minutes, 200 ℃	3.2155	3.0063	0.2092	1.1622×10^{-4}

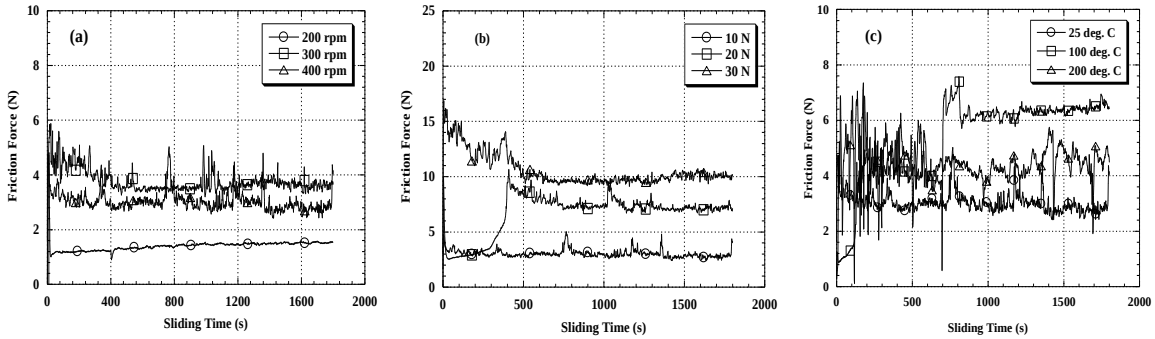

Fig. 6 Variations in friction force with sliding time during wear tests at different (a) sliding speeds (b) normal loads and (c) temperatures.

4. Conclusions

This paper investigates the compression, flexure and wear behaviours of Al6082-T6 alloy. Effects of strain rates and specimen geometry are observed under compression and flexure and thereafter, Johnson-Cook material model is evaluated based on the experimental data using curve fitting method. Following conclusions are drawn from the present investigation:

- The Al6082-T6 alloy is sensitive to compressive and flexural loads, i.e., the material properties change with changing loading rate.
- The energy dissipations in 50% compression of cylindrical specimens for *L/D* ratios 0.4, 0.8 and 1.2 varies nearly 165-212 MJ/m^3, 204-220 MJ/m^3 and 217-243 MJ/m^3 respectively in the strain rate range 0.0001-0.1 s^{-1}.
- In three-point bending, the energy dissipation for span length 150 mm varies nearly 76-80 MJ/m^3 at speeds 1-100 mm/min. In transverse orientation of flexural specimen of 150 mm span length, the energy dissipation increased by nearly 16% as compared to the flat orientation of the specimen at 100 mm/min speed.
- Johnson-Cook model can represent the flow stress of the alloy under compression and flexural loads.
- On increasing speed/load, the wear loss and wear rate increase. The maximum wear loss and wear rate are obtained at the maximum applied normal load (30 N), whereas the minimum wear loss and wear rate are found at maximum temperature (200 °C).

R E F E R E N C E S

[1]. *Y. Wang and Z. Jiang,* "Dynamic compressive behavior of selected aluminum alloy at low temperature", Materials Science and Engineering: A, 553, 2012, 176-180.

[2]. *D.P. Mondal, N. Jha, A. Badkul, S. Das, M.S. Yadav and P. Jain,* "Effect of calcium addition on the microstructure and compressive deformation behaviour of 7178 aluminium alloy", Materials & Design, 32 (5), 2011, 2803-2812.

[3]. *T. Ye, L. Li, P. Guo, G. Xiao and Z. Chen,* "Effect of aging treatment on the microstructure and flow behavior of 6063 aluminum alloy compressed over a wide range of strain rate", International Journal of Impact Engineering, 90, 2016, 72-80.

[4]. *Z. Lu, Q. Pan, X. Liu, Y. Qin, Y. He and S. Cao,* "Artificial neural network prediction to the hot compressive deformation behavior of Al–Cu–Mg–Ag heat-resistant aluminum alloy", Mechanics Research Communications, 38 (3), 2011, 192-197.

[5]. *Z. Wang, J. Shen, G. Lu and L. Zhao,* "Compressive behavior of closed-cell aluminum alloy foams at medium strain rates", Materials Science and Engineering: A, 528 (6), 2011, 2326-2330.

[6]. *E. Linul, N. Movahedi and L. Marsavina,* "The temperature and anisotropy effect on compressive behavior of cylindrical closed-cell aluminum-alloy foams", Journal of Alloys and Compounds, 740, 2018, 1172-1179.

[7]. *X. Xu, H. Zhao, Y. Hu, L. Zong, J. Qin, J. Zhang and J. Shao,* "Effect of hot compression on the microstructure evolution of aluminium bronze alloy", Journal of Materials Research and Technology, 19, 2022, 3760-3776.

[8]. *G. Prakash, N.K. Singh, P. Sharma and N.K. Gupta,* "Tensile, compressive, and flexural behaviors of Al5052-H32 in a wide range of strain rates and temperatures", Journal of Materials in Civil Engineering, 32(5), 2020, 04020090.

[9]. *G. Prakash, N.K. Singh and N.K. Gupta,* "Deformation behaviours of Al2014-T6 at different strain rates and temperatures", Structures, 26, 2020, 193-203.

[10]. *B. Li, Y. Wang, Z. Wang, X. Zhi, Y. Zhang and Y. Ouyang,* "7A04-T6 high-strength aluminium alloy SHS and RHS beams under pure bending—Testing, modelling and design recommendations", Thin-Walled Structures, 177, 2022, 109400.

[11]. *D. Zhang, S. Chen, Y. Lu and X. Chen,* "Quasi-static experimental study on flexural performance of aluminum-reinforced laminated glass beams", Engineering Structures, 256, 2022, 113993.

[12]. *S. Akram, A. Babutskyi, A. Chrysanthou, D. Montalvão, M.J. Whiting and N. Pizurova,* "Improvement of the wear resistance of nickel-aluminium bronze and 2014-T6 aluminium alloy by application of alternating magnetic field treatment", Wear, 480–481, 2021, 203940.

[13]. *A. M. Razzaq, D. L. Majid, M. R. Ishak and U. M. Basheer,* "Effects of Solid Fly Ash on Wear Behaviour of AA6063 Aluminum Alloy", Encyclopedia of Smart Materials, 1, 2019, 503-508.

[14]. *S. Sagar, N. K. Singh and N. S. Maurya,* "Strain rate behaviour and notch sensitivity of Aluminium 6082-T6 alloy under tensile loads", U.P.B. Sci. Bull. Series B, 85 (1), 2023, 201-212.

[15]. *N. K. Singh, E. Cadoni, M. K. Singha and N. K. Gupta,* "Dynamic tensile and compressive behaviors of mild steel at wide range of strain rates", Journal of Engineering Mechanics, 139 (9), 2013, 1197-1206.

[16]. *N. K. Singh, M. K. Singha, E. Cadoni and N. K. Gupta,* "Strain rate sensitivity of an aluminium alloy under compressive loads", Advanced Materials Research, 548, 2012, 169-173.

[17]. *G. Prakash, N. K. Singh, D. Kumar and P. Chandel,* "Compression and Flexure Behaviours of Magnesium Alloy AZ41 at different Strain Rates", UPB Scientific Bulletin, Series D: Mechanical Engineering, 82 (2), 2020, 211-222.

[18]. *E. Cadoni, N. K. Singh, D. Forni, M. K. Singha and N. K. Gupta,* "Strain rate effects on the mechanical behavior of two Dual Phase steels in tension", The European Physical Journal Special Topics, 225 (2), 2016, 409-421.

[19]. *O. S. Hopperstad, M. Langseth and T. Tryland,* "Ultimate strength of aluminium alloy outstands in compression: experiments and simplified analysis," Thin-Walled Structures, 34, 1999, 279–294.

[20]. *X. Qian, N. Parson and X. G. Chen,* "Effects of Mn addition and related Mn-containing dispersoids on the hot deformation behavior of 6082 aluminum alloys", Materials Science and Engineering: A, 764, 2019, 138253.

[21]. *N. Torić, J. Brnić, I. Boko, M. Brčić, I. W. Burgess and I. Uzelac,* "Experimental Analysis of the Behaviour of Aluminium Alloy EN 6082AW T6 at High Temperature", Metals, 7(4), 2017, 126, https://doi.org/10.3390/met7040126.

[22]. B. *Zhang and T. N. Baker,* Effect of the heat treatment on the hot deformation behaviour of AA6082 alloy. J. Mater. Process. Technol., 153–154, 2004, 881-885.

[23]. *F. Leoni, L. Sandness, Ø. Grong and F. Berto,* "Mechanical behavior of gas metal arc AA6082-T6 weldments", Procedia Structural Integrity, 18, 2019, 449-456.

[24]. *E. Troiani and N. Zavatta, "*The Effect of Laser Peening without Coating on the Fatigue of a 6082-T6 Aluminum Alloy with a Curved Notch", Metals 9, 2019, 728, doi:10.3390/met9070728.

[25]. *Y. Zhao and X. Zhai,* "Bending strength and design methods of the 6082-T6 aluminum alloy beams with circular hollow sections", Structures, 26, 2020, 870-887.

[26]. *A. Sert, S. Gürgen, O.N. Çelik and M. C. Kuşhan,* "Effect of heat treatment on the bending behavior of aluminum alloy tubes", Journal of Mechanical Science and Technology, 31 (11), 2017, 5273-5278.

[27]. *G. Prakash, N. K. Singh and N. K. Gupta,* "Flow behaviour of Ti-6Al-4V alloy in a wide range of strain rates and temperatures under tensile, compressive and flexural loads", International Journal of Impact Engineering, 176, 2023, 104549.

[28]. *M. K. Gupta, N. K. Singh and N. K. Gupta,* "Deformation behaviour and notch sensitivity of a super duplex stainless steel at different strain rates and temperatures", International Journal of Impact Engineering, 174, 2023, 104494.

[29]. *M. K. Gupta, N. K. Singh and N. K. Gupta,* "Energy dissipation and notch sensitivity of mild steel at different strain rates and temperatures", International Journal of Impact Engineering, 178, 2023, 104610.

[30]. *P. Sharma, D. Khanduja and S. Sharma,* "Dry sliding wear investigation of Al6082/Gr metal matrix composites by response surface methodology", Journal of Materials Research and Technology, 5(1), 2016, 29–36.

[31]. *T. Zhang and D. Y. Li,* "Improvement in the resistance of aluminum with yttria particles to sliding wear in air and in a corrosive medium", Wear, 251(1-12), 2001, 1250-1256.

[32]. *N. Yuvaraj,* "Improving the Wear Properties of Aluminum 6082 Alloy by Surface Compositing with ZrO2 Ceramic Particles Via Friction Stir Processing", Mat. Sci. Res. India, 15(1), 2018, http://dx.doi.org/10.13005/msri/150108.

[33]. *C. N. Panagopoulos, E. P. Georgiou and A. G. Gavras,* "Corrosion and wear of 6082 aluminum alloy", Tribology International, 42, 2009, 886-889.